Design and Modelling of an Enclosed Array of Square Spiral Antennas for Microwave Tomography

Milos Subotic[1,2], Nebojsa Pjevalica[1], Laszlo Palfi[2]

[1]*Department of Computing and Control Engineering, Faculty of Technical Sciences,*
University of Novi Sad,
Trg Dositeja Obradovica 6, 21000 Novi Sad, Serbia
[2]*RT-RK Institute for Computer Based Systems,*
Narodnog fronta 23a, 21000 Novi Sad, Serbia
milos.subotic@ uns.ac.rs

Abstract—**Microwave tomography is a microwave imaging method in which the resolution is not limited by wavelength, but rather by measurement noise and modelling errors. Inversion algorithm is used for obtaining an image from the measured scattered waves. Performance improvement of the inversion algorithm is introduced by approximately modelled antennas as a point, line or plane source. Such modelling of antennas introduces modelling errors. Antenna array in the unshielded measurement chamber will pick up external interference, as well as backscattering of array's own radiation. Multipath occurring in measurement chamber has a large impact on the measurement performance. The wave propagated through the air and reflected from the chamber walls could mask a weaker wave scattered by the object under imaging. Also, a larger number of the antennas improves inversion and gives a more accurate image. This paper proposes a novel design of enclosed measurement antenna array for microwave tomography. To obtain an accurate and efficient antenna model in 3D FDTD, a square spiral wire antenna is used in this design. A metal shield protects the process of measurement from external interference and backscattering. Between the antenna array and the metal shield an absorption wall is introduced, which decreases multipath and partially prevents signal masking. Square spiral wire antennas are overlapped and packed, giving a larger number of antennas in the same space. Enclosed antenna array is modelled in 3D FDTD. Proposed antenna array is compared with solutions found in literature. Comparison is done using metrics relevant for antenna array measurement in microwave tomography.**

Index Terms—**Microwave tomography; microwave imaging; antenna arrays; antenna modelling; antenna design; FDTD; square spiral antenna.**

I. INTRODUCTION

Microwave tomography (MWT) [1], [2] is a microwave imaging method for acquiring images from microwaves scattered by the object under imaging. MWT is a quantitative imaging method, where the image represents a map of dielectric properties. One of the antennas acts as the transmitter, illuminating the object, while the other antennas measure the scattered waves. In each iteration a different antenna is used as the transmitter, providing an additional point of view, acquiring more measurement data from different angles and positions. An image is obtained from the measurement by an inversion algorithm i.e. by searching for a map of dielectric properties which yields scattered waves in a simulation similar to the measured ones. A better match between simulated and measured waves gives a more realistic image of the object under imaging [1].

The forward solver, i.e. a numeric algorithm used in an inversion for scattering simulation, has a high computational cost, lasting for seconds [3] or even minutes [4]. The optimization algorithm evaluates the forward solver multiple times to find the optimal solution for a map of dielectric properties. To reduce the computational burden of the forward solver, usually some approximations in modelling are applied, for example Born approximation or regularization [5]–[8]. Also, many methods use an approximated model of transmit antennas including line source [7], [9] or a plane wave [1], [3], while instead of modelling receive antennas, the field is just sampled at the appropriate positions. Most imaging methods are 2D and ignore the 3D nature of wave propagation and scattering.

MWT, as an inverse problem, is inherently ill-conditioned, which means that a small change in measurement has a large impact on the resulting image. This makes MWT very sensitive to noise in measurement data. High conductivity values along with large permittivity contrast in the object of imaging results in a drastic attenuation of the scattered waves. Weak scattered waves could be easily masked by multipath waves traveling through the air. Measurement equipment acquires both strong multipath and weak scattered signals, where typically the weak scattered signal falls below noise floor.

The number of variables in inversion is proportional to the number of image pixels. A larger number of variables compared to the number of antennas makes this problem underestimated [10]. A larger number of measurement frequencies also improves inversion [7], [11].

Typical application of MWT is in biomedical imaging [2]. The non-ionizating nature of microwaves makes them relevant for tumour detection [8], [12]–[14], head imaging [15], extremity imaging [5], [6], tumour treatment [16]. For these reasons MWT is a promising research area.

Working in a near-field region, MWT image resolution is not limited by the wavelength of microwaves, as opposed to far-field and radar-based imaging methods. MWT manifests super-resolution properties [17], [18]. Currently, the only known limitations for image quality and resolution are noise and modelling errors [17].

Many research papers tackle the problem of accurate antenna modelling [9], [19]–[22], promising better imaging with more accurate models. Antenna array design is the subject of many works [5], [8], [11], [15], [23]–[25], just to name some.

Accurate modelling of antenna array is a computation and memory intensive task, having a large number of antennas surrounding the object under imaging. Scattered fields are measured with S-parameters, while the forwards solver in simulation records field values. This produces difficulties in conversion between measured and simulated data. The usual method for creating conversion function is calibration [11], [23], [24]. A recently introduced source reconstruction method [26] creates comparable qualitative conversion function, requiring no calibration. For an approximated antenna model to work, adjacent antennas should be distanced far enough to have low mutual coupling [11]. A larger distance between antennas limits their number in the array, having impact on the imaging quality.

Monopole [19], [24] and dipole [5], [6] antennas, could be easily modelled. A disadvantage of such antennas is their omnidirectional radiation pattern in the imaging plane, which increases mutual coupling. This degrades measured field signal fidelity [27] and degradates overall imaging quality [22].

Practically, all solutions have a measurement chamber filled with lossy matching fluid, instead of air as the background medium. One purpose of the matching fluid is lowering contrast between the skin and the background, making less reflection from the skin and higher transmission into the body. Inversion methods based on Born approximation work properly only if the aforementioned contrast is low. Another purpose of the lossy matching fluid is lowering multipath effect and signal masking. While the primary wave propagates through the tissues, the secondary wave propagates through the lossy fluid resulting in attenuation comparable to the primary one. Additional losses in front of and behind the object under imaging require stronger transmitters and more sensitive measurement equipment. On the other hand, the matching fluid could be uncomfortable and complicates antenna array and imaging chamber design. The solution proposed in this paper avoids the use of matching fluid, and solves aforementioned problems using an absorption wall.

The antenna array proposed in this paper is modelled in a 3D Cartesian grid and simulated with a Finite-Difference Time-Domain (FDTD) method [28]. The geometry of the antennas and the imaging chamber is rectangular and discretized on a coarse grid. An Archimedean square spiral wire antenna [29], [30] matches the aforementioned geometry of the grid. This antenna is perpendicular to the direction of radiation, occupying less volume in the simulation space and making modelling more efficient. An additional benefit of the spiral antenna is ultrawide bandwidth.

The proposed antenna solution, as a wire antenna without substrate, has low Radar Cross-Section (RCS). Low RCS means low reflection i.e. high transparency, enabling the placement of antennas one behind the other. The overlapping of antennas in such a way enables a larger number of antennas in the same area.

As mentioned before, the measurement chamber is protected by a metal shield and an absorption wall is placed between the shield and the antenna array. The wall absorbs the waves which would otherwise reflect from the metal shield. The wall has low permittivity for low reflection, and high conductivity for high loss.

The model of antenna array presented in this paper could be used as the forward solver in the inverse algorithm. Since the model could faithfully reflect the built antenna array, this solution could give high performances.

Two antenna array designs with multiple configurations are simulated and compared using metrics relevant for MWT: computation and memory performance, radiation from the chamber and fidelity of the measured signal.

Chapter II describes the design and the modelling of antenna array in details. The metrics and the simulation results are presented in Chapter III. Chapter IV gives final conclusions and includes future research directions.

II. ANTENNA ARRAY DESIGN

A. Antenna Design Methodology

In this work, the openEMS framework [31] is used for array modeling. openEMS is a 3D Equivalent Circuit FDTD (EC-FDTD) [32] and has the feature of modelling lumped elements. This feature enables direct recording of S-parameters of simulated antennas, potentially avoiding aforementioned complex calibration methods found in [11], [23], [24]. Also, openEMS is fast and parallelized FDTD implementation.

As mentioned before, to ensure accurate modelling in FDTD it is necessary to model antenna array geometry in a 3D Cartesian grid. Every wire, metal sheet or edge of absorber wall should be aligned to the grid lines. For efficient modelling, coarse grid discretization is needed. The Vivaldi antenna commonly used in MWT [11], [33], [34] needs a very fine grid for accurate curve representation. Even if the antenna geometry is rectangular, too irregular geometry, as in [35], could make the grid too dense, making modelling inefficient. The openEMS FDTD simulator used in this work has a graded grid, so there is no need for completely regular geometry.

Typically, antennas in the array are placed in a circular ring, [15], [23] with few exceptions of square ring placement [36], [37]. Placement of the antennas in a square ring allows modelling of an array in Cartesian grid. Square ring placement is used in this paper as well.

It is also necessary to select a low profile antenna i.e.

antenna which is perpendicular to the direction of radiation, as mentioned before. Such an antenna would occupy less volume compared to the aforementioned Vivaldi and waveguide antennas [15].
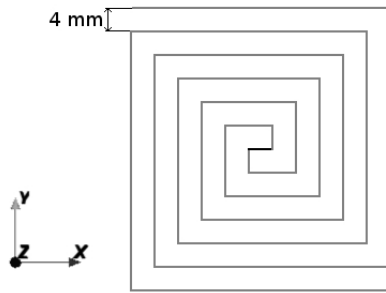

Fig. 1. Designed square spiral antenna.

A similar methodology of rectangular geometry is used for designing an array based on the multiband patch antenna [8], [14], [37], [38]. This array successfully fulfills all the aforementioned criteria, In [37], some additional criteria are given, for example possibility of coregistration with Magnetic Resonance Imaging (MRI).

For the purpose of this paper, an Archimedean square spiral wire antenna is used. The antenna is shown in Fig. 1. In this work, a wire antenna is placed in a 4 mm×4 mm×4 mm grid. Both spiral arms have 12 segments which cover the overall area of 44 mm×48 mm.

The grid resolution of 4 mm is a compromise between performance and the antenna's directionality and impedance. Directionality is higher and flatter with a finer grid, while impedance is flatter and lower. On the other side, computational and memory resources have cubic growth with grid resolution growth.

The spiral antenna is a wideband antenna. The perimeter of the spiral antenna should be at least $1.25\lambda_{max}$ [29], where λ_{max} is the wavelength of the lowest working frequency. The distance between feed points should be less than $\lambda_{min}/4$, where λ_{min} is the wavelength of the highest working frequency. As mentioned before, wide bandwidth is beneficial in MWT. The frequency range of this antenna is from 2 GHz to 18 GHz. In FDTD, the antenna's response is measured in a range of 2 GHz to 3 GHz. Higher frequencies are not useful for MWT because of high losses, and the recommended frequency range should be 0.5 GHz to 3 GHz [37].

In previous work [39] this particular antenna selection and design methodology is elaborated in more details. In the same paper, a detailed comparison between the proposed square spiral antenna and multiband patch antenna from [37] is given, including comparison of radiation patterns and gain.

B. Array Design and Modelling

The proposed wire antenna has low RCS and high transparency, as mentioned before. This property is used for spiral antenna overlapping. When overlapped, the antennas occupy less area in comparison with non-overlapped antennas. The scheme for overlapping is placing the antennas 2 by 2 in four layers, avoiding contact between

wires, occupying space five cells thick. This scheme is repetitive, so any number of antennas could be placed in no more than four layers. Overlapping of four antennas is shown in Fig. 2. For stability, a material with low permittivity and dielectric losses could be placed between these four antenna layers. An example of such material is Styrofoam.
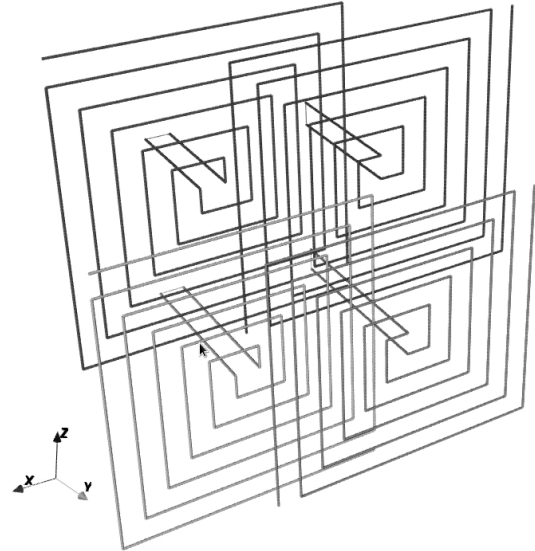

Fig. 2. Overlapping wire antennas.

Even if occupying a larger area than 28 mm×29 mm as the previously mentioned multiband patch [37], many more spiral antennas could be placed in the same space when overlapped. The aforementioned arrays from [8], [14], [37] are placed in a cubical chamber with dimensions ranging from 15 cm to 16 cm. These arrays have 32 patch antennas, 8 per each one of the 4 vertical sides. For this work, a chamber of similar dimensions as aforementioned one is designed and has 100 antennas, 5×5 per side.

The main limitation when overlapping antennas assumes avoiding contact between wires. This limitation rises from a limited Perfect Electric Conductor (PEC) wire model in the FDTD. A better wire model could enable an even better overlapping scheme [40]. With a better overlapping scheme it is possible to implement larger antennas which would also cover lower frequencies beneficial for inversion. Additionally, another limitation of PEC wire model is its ability to model only thick wires. Implementing a thin-wire model in the FDTD like [40], [41] would enable modelling of the wire with more realistic thickness.

As described earlier, instead of the lossy matching fluid an absorption wall is used for decreasing multipath and signal masking. The absorption wall is placed between array of the overlapping antennas and the metal shield. The absorption wall attenuates the waves propagating from the chamber interior towards the metal shield. Wave reflection from the metal shield could create multipath, but because it is attenuated by the absorption wall, its impact is less severe. Low permittivity of the absorption wall directly causes low reflection. In this way, receive antennas which are in line of sight with the transmit antenna, are not protected from signal masking. This is the main disadvantage, but if the object under imaging is large enough, the number of such antennas

will be low. The main advantage is the lack of strong transmitters and sensitive receivers required, as is the case with systems with lossy fluid. An additional signal amplification is needed to compensate additional attenuation through the lossy fluid in the front of and behind the object under imaging. This is not needed in the proposed solution with absorption because waves in the same space travel through the air without attenuation.
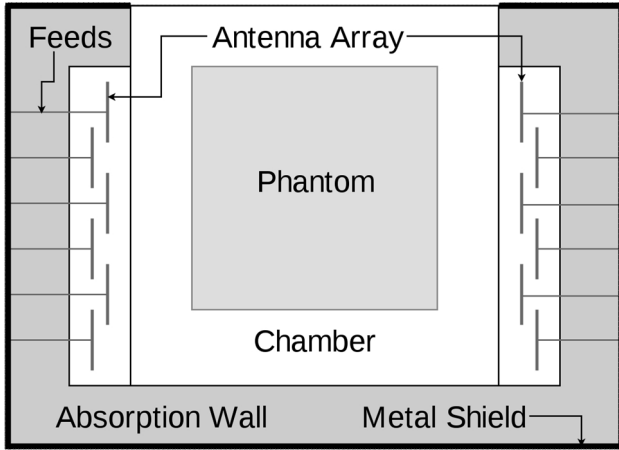

Fig. 3. Construction of the proposed chamber.

A balsa wood is selected as the material for the absorption wall. Balsa wood has low permittivity and high dielectric loss. Wall is 2 cm thick. In this work, balsa wood is modeled with $\varepsilon_r = 1.22$ and $\tan\delta = 0.1$ at 3 GHz [42]. In literature dielectric parameters for balsa wood are not consolidated, so measurements of samples are needed [43]. Dielectric parameters change over a frequency, so a better dielectric model should be used, like Lorentz or Debye. One advantage of balsa wood is zero permeability i.e. $\mu_r = 0$. This is beneficial when implementing FDTD, because the lack of modelling permeability boosts performances. Other materials with similar characteristics found in literature are Nylon, rice husk with coal [44] and other kind of wood material. Typical absorbers used in an anechoic chamber are based on magnetic materials.

As described earlier, each of the four vertical sides is composed of a metal shield, an absorption wall and an antenna array. The feeds of antennas are twin parallel wires snapped to the grid stretched from the antenna up to the shield. The bottom of the chamber is closed by the absorption wall and the shield. The top side has a similar cover over the horizontal layered wall of balsa and antennas, leaving a square hole above the chamber. This decreases emitting waves outside the chamber, as well as lowering external interference. For purposes of signal fidelity testing, to recreate multipath and the signal masking problem, an object is placed inside the chamber. This object, called phantom, could be an anatomically realistic part of the body [3], [10] or could be some simple geometric shape, appearing as part of the body. For purposes of testing proposed solution, a simple cuboid object with dielectric properties similar to tissue is used. Fig. 3 shows the cross-section of the chamber with the phantom. For comparison purposes, the proposed chamber could be filled with air or lossy matching fluid with complex permittivity $76-14i$ [6].

Also, the absorption wall could be removed and the bottom side could be opened in a similar way as the top. Around chamber 8 Perfectly Matched Layer (PML) layers are used.

III. RESULTS

For the proposed square spiral antenna array three test configurations were made. The first assumes a chamber without an absorption wall and without the matching fluid. The second assumes the matching fluid only, while the third is with the absorption wall only. These configurations are prepared for comparison of the different methods for solving multipath and the signal masking problem. Additionally, a multiband patch antenna array [37] is modelled, as the state of the art solution. Single configuration is used, with matching fluid. All configurations have simple phantom used.

The first metric for comparison is computation and memory performance. Table I presents the mesh information and comparison of two modelled antenna arrays by efficiency. The columns represent the mesh resolution (Min Δ), the volume in mesh cells (Mesh vol), the number of timestamps for simulation (Sim steps), the summary cost of the model presented as a product of mesh volume with the number of timestamps for simulation (Mesh cost), respectively. Memory resources needed for the modelling of each enclosed array are proportional to the mesh volume, while the computational resources are directly proportional to the mesh cost.

TABLE I. COMPARISON OF GEOMETRY AND PERFORMANCES.

Metric	Min Δ	Mesh vol	Sim steps	Mesh cost
Unit	mm	cells	steps	cells×steps
Spiral	4	37653	273829	1.0×10^{10}
Spiral fluid	4	4837	273829	1.3×10^{9}
Spiral absorber	4	9884	388125	3.8×10^{9}
Patch fluid	1	21902	1191300	2.6×10^{10}

From Table I it can be seen that the proposed solution with the absorption wall is more computational and memory demanding than the solution with the matching fluid. The reasons for that lies in an additional number of cells for the absorption wall and longer energy fading time. The chamber without wave attenuation of any type has, on the other hand, very long fading time, because all waves need to escape the chamber through the top opening. Multiband patch array has higher performance cost because of finer resolution and lower timestep.

As the space outside the chamber is not modelled, backscattering through the opening on top side of measurement chamber could produce difficulties for inversion algorithm. Backscattering through this opening is proportional to the radiation from the same opening. Radiation through this hole could be decreased by using antennas with higher directivity and with absorption of outgoing waves by lossy matching fluid. This radiation could be measured by the common methods for the antenna radiation efficiency measurement. Radiation efficiency is defined as ratio of radiated power over input power. In this work, lower values of radiation efficiency are better.

Radiation efficiency for proposed array without attenuation, with matching fluid, with absorption wall, multiband patch array with matching fluid are 1.6553×10^{-2}, 1.0370×10^{-7}, 1.5661×10^{-2}, 6.0588×10^{-8}, respectively. It could be concluded that the lossy matching fluid largely attenuates outgoing radiation, but at the cost of decreased signal strength.
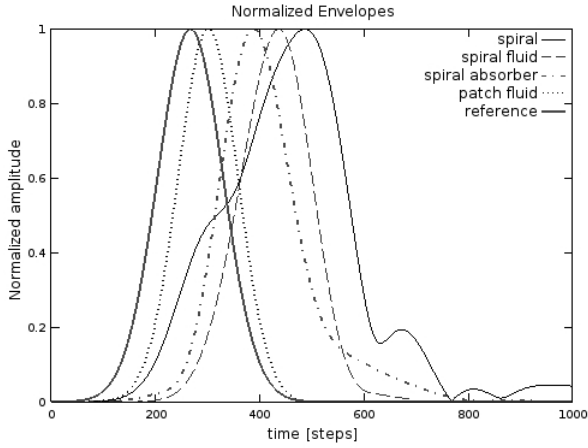

Fig. 4. Normalized envelopes of measured signals.

Most important metric is signal fidelity [27], [45]. Fidelity could be defined as similarity between measured signal and excitation signal. Multipath produces signal masking and measured signal is distorted in contrast with excitation signal. In this paper fidelity is measured by cross-correlation between excitation and measured signal of the different configurations.

Both chambers are excited with signal having carrier frequency of 2 GHz and -20 dB bandwidth set to 200 MHz. Antenna in the centre of one vertical side is used as transmitter, while opposite antenna is used for measurement. The phantom is in line of sight between these antennas. This setup tries to recreate signal masking scenario. Envelope of the measured signal is calculated by Hilbert transform (MATLAB function *hilbert()*), for easier visualization. Note that Hilbert transform could extract envelope with enough precision, because bandwidth is narrow in comparison with carrier.

Fig. 4 presents normalized envelopes of proposed array without attenuation, with matching fluid, with absorption wall, multiband patch array with matching fluid, and reference excitation signal (Gaussian), respectively. It could be seen that chamber without any attenuation has extensive multipath, reflected in many bumps occurring on the signal. Also, it could be noticed that array with absorption wall has thicker tail because slower energy decay, utilizing longer simulation time. On the other hand, square spiral array with matching fluid has signal leaned to the right. Maximum amplitudes of these envelopes are 8.1467×10^{-5}, 1.9317×10^{-7}, 9.0957×10^{-5}, 4.9049×10^{-7} and 2.0005×10^{-2}. It could be noticed that solution with absorption wall has higher amplitude values in contrast with lossy matching fluid solution.

Additionally, a cross-correlation between these signals is calculated (MATLAB function *corr()*). Result is matrix of the correlation coefficients, shown in Table II. Each row and column refers to its respective configuration (by the same order as in Fig. 4). Cell in the intersection between row and column is a correlation coefficient, which results with a matrix symmetry. Higher values indicate matching (1.0 is a complete match), while lower values indicate mismatching between signals (0.0 is a complete mismatch). Last column represents correlation between signals from Fig. 4 and a reference signal. Patch array solution exposes best match with reference signal, having highest value in 4th field of the last column (5th field with 1.0 is comparison of reference signal with itself). Spiral array with absorption wall and a configuration without any absorption has moderate matching (1st and 3rd fields), while spiral array with lossy fluid has lowest matching with reference signal (2nd field).

TABLE II. CORRELATION COEFFICIENTS BETWEEN NORMALIZED ENVELOPES.

Chamber configurations	Spiral	Spiral fluid	Spiral absorber	Patch fluid	Reference
Spiral	1.000	0.897	0.823	0.431	0.338
Spiral fluid	0.897	1.000	0.917	0.317	0.183
Spiral absorber	0.823	0.917	1.000	0.543	0.347
Patch fluid	0.431	0.317	0.543	1.000	0.919
Reference	0.338	0.183	0.347	0.919	1.000

The problem with the aforementioned cross-correlation based fidelity metric is exposed in its inability to answer the question: how the introduced features impact inversion performance and final image quality. A more advanced method is Truncated Singular Value Decomposition (TSVD) [38], [46]. TSVD method separates the testing of measured data quality from the problem of the inversion algorithm design.

IV. CONCLUSIONS

This paper offers a novel design of overlapped square spiral antenna array enclosed with an absorption wall and a metal shield. Instead of approximated 2D modelling, antennas are modelled in 3D, which reduces modelling error, making appropriate base for generation of better final images. Also, modelled chamber is shielded, making it immune to external interference sources. Most significant novelty presented in this paper is absorption wall for decreasing multipath along with overlapped square spiral antennas. The modelled array is simulated and compared using several proposed metrics, but further improvements and measurement are needed for final conclusions. It is shown by simulation that proposed solution with the lossy matching fluid has better computing performance, yet the solution with the absorption wall exposes slightly better measured signal fidelity. Additionally, a higher number of antennas and wider bandwidth of proposed array promise faster inversion and better imaging results.

Future research direction would be focused on updating material and thin-wire models, developing better overlapping scheme and usage of more realistic phantoms. Furthermore, the proposed array will be tested with the TSVD method, as more advance metric used in literature. The final task assumes building the proposed enclosed antenna array, followed by the comparison with its model.

REFERENCES

[1] S. Noghanian, A. Sabouni, T. Desell, A. Ashtari, *Microwave Tomography: Global Optimization, Parallelization and Performance Evaluation*. Springer Publishing Company, Incorporated, 2014. [Online]. Available: https://doi.org/10.1007/978-1-4939-0752-6

[2] R. Chandra, H. Zhou, I. Balasingham, R. M. Narayanan, "On the opportunities and challenges in microwave medical sensing and imaging", *IEEE Transactions on Biomedical Engineering*, vol. 62, no. 7, pp. 1667–1682, 2015. [Online]. Available: https://doi.org/10.1109/tbme.2015.2432137

[3] A. Sabouni, S. Noghanian, S. Pistorius, "A global optimization technique for microwave imaging of the inhomogeneous and dispersive breast", *Canadian Journal of Electrical and Computer Engineering*, vol. 35, no. 1, pp. 15–24, 2010. [Online]. Available: https://doi.org/10.1109/cjece.2010.5783380

[4] M. Donelli, I. J. Craddock, D. Gibbins, M. Sarafianou, "A threedimensional time domain microwave imaging method for breast cancer detection based on an evolutionary algorithm", *Progress in Electromagnetics Research M*, vol. 18, pp. 179–195, 2011. [Online]. Available: https://doi.org/10.2528/pierm11040903

[5] C. Gilmore, A. Zakaria, S. Pistorius, J. LoVetri, "Microwave imaging of human forearms: Pilot study and image enhancement", *International Journal of Biomedical Imaging*, vol. 2013, pp. 1–17, 2013. [Online]. Available: https://doi.org/10.1155/2013/673027

[6] M. Ostadrahimi, P. Mojabi, A. Zakaria, J. LoVetri, L. Shafai, "Enhancement of Gauss–Newton inversion method for biological tissue imaging", *IEEE Transactions on Microwave Theory and Techniques*, vol. 61, no. 9, pp. 3424–3434, 2013. [Online]. Available: https://doi.org/10.1109/tmtt.2013.2273758

[7] J. D. Shea, P. Kosmas, S. C. Hagness, B. D. Van Veen, "Threedimensional microwave imaging of realistic numerical breast phantoms via a multiple-frequency inverse scattering technique", *Medical physics*, vol. 37, no. 8, pp. 4210–4226, 2010. [Online]. Available: https://doi.org/10.1118/1.3443569

[8] M. J. Burfeindt, N. Behdad, B. D. Van Veen, S. C. Hagness, "Quantitative microwave imaging of realistic numerical breast phantoms using an enclosed array of multiband, miniaturized patch antennas", *IEEE Antennas and Wireless Propagation Letters*, vol. 11, pp. 1626–1629, 2012. [Online]. Available: https://doi.org/10.1109/lawp.2012.2236071

[9] M. Ostadrahimi, P. Mojabi, C. Gilmore, A. Zakaria, S. Noghanian, S. Pistorius, J. LoVetri, "Analysis of incident field modeling and incident/scattered field calibration techniques in microwave tomography", *IEEE Antennas and Wireless Propagation Letters*, vol. 10, pp. 900–903, 2011. [Online]. Available: https://doi.org/10.1109/lawp.2011.2166849

[10] F. Bai, A. Franchois, A. Pizurica, "3D microwave tomography with huber regularization applied to realistic numerical breast phantoms", *Progress in Electromagnetics Research*, vol. 155, pp. 75–91, 2016. [Online]. Available: https://doi.org/10.2528/pier15121703

[11] C. Gilmore, P. Mojabi, A. Zakaria, M. Ostadrahimi, C. Kaye, S. Noghanian, L. Shafai, S. Pistorius, J. LoVetri, "A wideband microwave tomography system with a novel frequency selection procedure", *IEEE Transactions on Biomedical Engineering*, vol. 57, no. 4, pp. 894–904, 2010. [Online]. Available: https://doi.org/10.1109/tbme.2009.2036372

[12] P. M. Meaney, M. W. Fanning, D. Li, S. P. Poplack, K. D. Paulsen, "A clinical prototype for active microwave imaging of the breast", *IEEE Transactions on Microwave Theory and Techniques*, vol. 48, no. 11, pp. 1841–1853, 2000. https://doi.org/10.1109/22.883861

[13] N. Epstein, P. Meaney, and K. Paulsen, "3D parallel-detection microwave tomography for clinical breast imaging", *Review of Scientific Instruments*, vol. 85, no. 12, p. 124704, 2014. [Online]. Available: https://doi.org/10.1063/1.4901936

[14] S. Aguilar, M. Al-Joumayly, J. Shea, N. Behdad, S. Hagness, "Design of a microwave breast imaging array composed of dual-band miniaturized antennas", in *2011 XXXth URSI General Assembly and Scientific Symposium*, IEEE, 2011. [Online]. Available: https://doi.org/10.1109/ursigass.2011.6051369

[15] S. Semenov, R. Planas, M. Hopfer, A. Hamidipour, A. Vasilenko, E. Stoegmann, E. Auff, "Electromagnetic tomography for brain imaging: Initial assessment for stroke detection", in *2015 IEEE Biomedical Circuits and Systems Conference (BioCAS)*, IEEE, 2015. [Online]. Available: https://doi.org/10.1109/biocas.2015.7348385

[16] J. Stang, M. Haynes, P. Carson, M. Moghaddam, "A preclinical system prototype for focused microwave thermal therapy of the breast", *IEEE Transactions on Biomedical Engineering*, vol. 59, no. 9, pp. 2431–2438, 2012. [Online]. Available: https://doi.org/10.1109/tbme.2012.2199492

[17] C. Gilmore, P. Mojabi, A. Zakaria, S. Pistorius, J. LoVetri, "On super-resolution with an experimental microwave tomography system", *Antennas and Wireless Propagation Letters, IEEE*, vol. 9, pp. 393–396, 2010. [Online]. Available: https://doi.org/10.1109/lawp.2010.2049471

[18] T. J. Cui, W. C. Chew, X. X. Yin, W. Hong, "Study of resolution and super resolution in electromagnetic imaging for half-space problems", *IEEE Transactions on Antennas and Propagation*, vol. 52, no. 6, pp. 1398–1411, 2004. [Online]. Available: https://doi.org/10.1109/tap.2004.829847

[19] E. A. Attardo, A. Borsic, G. Vecchi, P. M. Meaney, "Whole-system electromagnetic modeling for microwave tomography", *IEEE Antennas and Wireless Propagation Letters*, vol. 11, pp. 1618–1621, 2012. [Online]. Available: https://doi.org/10.1109/lawp.2013.2237745

[20] S. Padhi, A. Fhager, M. Persson, J. Howard, "Measured antenna response of a proposed microwave tomography system using an efficient 3-D FDTD model", *IEEE Antennas and Wireless Propagation Letters*, vol. 7, pp. 689–692, 2008. [Online]. Available: https://doi.org/10.1109/lawp.2008.2009888

[21] M. Holman, S. Noghanian, "Near-field excitation modeling in microwave tomography", in *IEEE International Conference on Electro/Information Technology* (EIT 2013), IEEE, 2013. [Online]. Available: https://doi.org/10.1109/eit.2013.6632689

[22] N. Bayat, P. Mojabi, "The effect of antenna incident field distribution on microwave tomography reconstruction", *Progress In Electromagnetics Research*, vol. 145, pp. 153–161, 2014. [Online]. Available: https://doi.org/10.2528/pier14021905

[23] P. Mojabi, M. Ostadrahimi, L. Shafai, J. LoVetri, "Microwave tomography techniques and algorithms: A review", in *15 International Symposium on Antenna Technology and Applied Electromagnetics 2012*, IEEE, 2012. [Online]. Available: https://doi.org/10.1109/antem.2012.6262367

[24] A. Fhager, S. K. Padhi, M. Persson, J. Howard, "Antenna modeling and reconstruction accuracy of time domain-based image reconstruction in microwave tomography", *International Journal of Biomedical Imaging*, vol. 2013, pp. 1–14, 2013. [Online]. Available: https://doi.org/10.1155/2013/343180

[25] D. J. Pagliari, A. Pulimeno, M. Vacca, J. A. Tobon, F. Vipiana, M. R. Casu, R. Solimene, L. P. Carloni, "A low-cost, fast, and accurate microwave imaging system for breast cancer detection", in *2015 IEEE Biomedical Circuits and Systems Conference (BioCAS)*, IEEE, 2015. [Online]. Available: https://doi.org/10.1109/biocas.2015.7348444

[26] C. Narendra, I. Jeffrey, P. Mojabi, "Using the source reconstruction method to model incident fields in microwave tomography." IEEE Antennas and Wireless Propagation Letters, vol. 16, pp. 46–49, 2017. [Online]. Available: https://doi.org/10.1109/lawp.2016.2554059

[27] A. T. Mobashsher, A. Abbosh, "Performance of directional and omnidirectional antennas in wideband head imaging", *IEEE Antennas and Wireless Propagation Letters*, vol. 15, pp. 1618–1621, 2016. [Online]. Available: https://doi.org/10.1109/lawp.2016.2519527

[28] A. Taflove, S. Hagness, *Computational Electrodynamics: The Finite-difference Time-domain Method*, ser. Antennas and Propagation Library. Artech House, 2000. [Online]. Available: https://books.google.com/books?id=F61iQgAACAAJ

[29] U. Saynak, "Novel rectangular spiral antennas", Ph.D. dissertation, Izmir Institute of Technology, 2007. [Online]. Available: http://library.iyte.edu.tr/tezler/master/elektrikveelektronikmuh/T000744.pdf

[30] U. Saynak, A. Kustepeli, "Novel square spiral antennas for broadband applications", *Frequenz*, vol. 63, no. 1-2, pp. 14–19, 2009. [Online]. Available: https://doi.org/10.1515/freq.2009.63.1-2.14

[31] T. Liebig, A. Rennings, S. Held, D. Erni, "openEMS –a free and open source equivalent-circuit (EC) FDTD simulation platform supporting cylindrical coordinates suitable for the analysis of traveling wave MRI applications", *International Journal of Numerical Modelling: Electronic Networks, Devices and Fields*, vol. 26, no. 6, pp. 680–696, 2012. [Online]. Available: https://doi.org/10.1002/jnm.1875

[32] A. Rennings, A. Lauer, C. Caloz, I. Wolff, "Equivalent circuit (EC) FDTD method for dispersive materials: derivation, stability criteria and application examples", in *Time Domain Methods in Electrodynamics*, Springer, 2008, pp. 211–238. [Online]. Available: https://doi.org/10.1007/978-3-540-68768-9_14

[33] M. Ostadrahimi, S. Noghanian, L. Shafai, A. Zakaria, C. Kaye, J. LoVetri, "Investigating a double layer Vivaldi antenna design for fixed array field measurement", *International Journal of Ultra Wideband Communications and Systems*, vol. 1, no. 4, pp. 282–290, 2010. [Online]. Available: https://doi.org/10.1504/ijuwbcs.2010.034309

[34] J. Bourqui, M. Okoniewski, E. C. Fear, "Balanced antipodal Vivaldi antenna with dielectric director for near-field microwave imaging", *IEEE Transactions on Antennas and Propagation*, vol. 58, no. 7, pp. 2318–2326, 2010. [Online]. Available: https://doi.org/10.1109/tap.2010.2048844

[35] J. W. Jayasinghe, J. Anguera, D. N. Uduwawala, "A high-directivity microstrip patch antenna design by using genetic algorithm optimization", *Progress In Electromagnetics Research C*, vol. 37, pp. 131–144, 2013. [Online]. Available: https://doi.org/10.2528/pierc13010805

[36] Z. Q. Zhang, Q. H. Liu, C. Xiao, E. Ward, G. Ybarra, W. T. Joines, "Microwave breast imaging: 3-D forward scattering simulation", *IEEE Transactions on Biomedical Engineering*, vol. 50, no. 10, pp. 1180–1189, 2003. [Online]. Available: https://doi.org/10.1109/tbme.2003.817634

[37] S. M. Aguilar, M. A. Al-Joumayly, M. J. Burfeindt, N. Behdad, S. C. Hagness, "Multiband miniaturized patch antennas for a compact, shielded microwave breast imaging array", *IEEE Transactions on Antennas and Propagation*, vol. 62, no. 3, pp. 1221–1231, 2014. [Online]. Available: https://doi.org/10.1109/tap.2013.2295615

[38] R. O. Mays, N. Behdad, S. C. Hagness, "A TSVD analysis of the impact of polarization on microwave breast imaging using an enclosed array of miniaturized patch antennas", *IEEE Antennas and Wireless Propagation Letters*, vol. 14, pp. 418–421, 2015. [Online]. Available: https://doi.org/10.1109/lawp.2014.2365755

[39] M. Subotic, L. Palfi, N. U. Pjevalica, "Efficient antenna modeling method for microwave tomography", in *2016 24th Telecommunications Forum Telfor (TELFOR)*, IEEE, 2016. [Online]. Available: https://doi.org/10.1109/telfor. 2016.7818828

[40] C. Guiffaut, A. Reineix, B. Pecqueux, "New oblique thin wire formalism in the FDTD method with multiwire junctions", *IEEE Transactions on Antennas and Propagation*, vol. 60, no. 3, pp. 1458–1466, 2012. [Online]. Available: https://doi.org/10.1109/tap.2011.2180304

[41] D. Kuklin, "Extension of thin wire techniques in the FDTD method for Debye media", *Progress in Electromagnetics Research M*, vol. 51, pp. 9–17, 2016. [Online]. Available: https://doi.org/10.2528/pierm16081804

[42] T. A. Kumar, J. Inayathullah, V. A. Nagarajan, S. H. Kumar, "Development of hybrid composite radar wave absorbing structure for stealth applications", *Bulletin of Materials Science*, vol. 39, no. 1, pp. 279–284, 2016. [Online]. Available: https://doi.org/10.1007/s12034-015-1133-3

[43] R. Olmi, M. Bini, A. Ignesti, C. Riminesi, "Dielectric properties of wood from 2 to 3 GHz", *Journal of Microwave Power and Electromagnetic Energy*, vol. 35, no. 3, pp. 135–143, 2000. [Online]. Available: https://doi.org/10.1080/08327823.2000. 11688430

[44] H. Kaur, G. D. Aul, V. Chawla, "Enhanced reflection loss performance of square based pyramidal microwave absorber using rice huskcoal", *Progress in Electromagnetics Research M*, vol. 43, pp. 165–173, 2015. [Online]. Available: https://doi.org/10.2528/pierm15072603

[45] A. T. Mobashsher, A. M. Abbosh, Y. Wang, "Microwave system to detect traumatic brain injuries using compact unidirectional antenna and wideband transceiver with verification on realistic head phantom", *IEEE Transactions on Microwave Theory and Techniques*, vol. 62, no. 9, pp. 1826–1836, 2014. [Online]. Available: https://doi.org/10.1109/tmtt.2014.2342669

[46] J. D. Shea, B. D. Van Veen, S. C. Hagness, "A TSVD analysis of microwave inverse scattering for breast imaging", *IEEE Transactions on Biomedical Engineering*, vol. 59, no. 4, pp. 936–945, 2012. [Online]. Available: https://doi.org/10.1109/tbme.2011.2176727